Available online at www.sciencedirect.com
ScienceDirect
Phytochemistry 69 (2008) 276–287
PHYTOCHEMISTRY
www.elsevier.com/locate/phytochem

Cytotoxic *ent*-abietane diterpenes from *Gelonium aequoreum*

Chia-Lin Lee [a], Fang-Rong Chang [a], Pei-Wen Hsieh [a], Michael-Y. Chiang [b], Chin-Chung Wu [a], Zih-You Huang [a], Yu-Hsuan Lan [a], Mei Chen [a], Kuo-Hsiung Lee [c], Hsin-Fu Yen [d], Wen-Chun Hung [e], Yang-Chang Wu [a,e,*]

[a] *Graduate Institute of Natural Products, Kaohsiung Medical University, Kaohsiung 807, Taiwan*
[b] *Department of Chemistry, National Sun Yat-Sen University, Kaohsiung 804, Taiwan*
[c] *Natural Products Research Laboratories, School of Pharmacy, The University of North Carolina at Chapel Hill, NC 27599, USA*
[d] *National Museum of Natural Science, Taichung, 404, Taiwan*
[e] *National Sun Yat-Sen University-Kaohsiung Medical University Joint Research Center, Kaohsiung 804, Taiwan*

Received 2 August 2006; received in revised form 27 April 2007
Available online 21 August 2007

Abstract

Seventeen *ent*-abietane diterpenes, including gelomulides K–X (**1**–**14**), and three known compounds, were isolated from a dichloromethane-soluble extract of *Gelonium aequoreum* through bioassay-guided fractionation. Their structures were identified by spectroscopic methods, and stereochemistry was confirmed by X-ray crystallographic analysis, CD spectral data, and Mosher's method. The isolates were evaluated for *in vitro* cytotoxic activity, and compounds **1** and **3** showed moderate cytotoxicity against lung (A549), breast (MDA-MB-231 and MCF7), and liver (HepG2) cancer cell lines.

Keywords: *Gelonium aequoreum*; Euphorbiaceae; *ent*-Abietane diterpenes; Gelomulides K–X; Cytotoxicity

1. Introduction

Gelonium, a genus of shrubs and small trees belonging to the Euphorbiaceae, is distributed in the tropical and subtropical parts of Asia and Africa. This genus contains about 25 species, but only one, *G. aequoreum*, is native to Taiwan (Chen et al., 1993). Thirty-three natural products, including 23 *ent*-abietane diterpenes, one diterpene lactone, four *entb*-kaurane diterpenes, two triterpenes, and three flavonoids, have been reported from this genus (Chakravarty et al., 1991; Choudhary et al., 2004; Das et al., 1993,1994; Jahan et al., 2002, 2004; Parveen and Khan, 1987; Row and Rao, 1969; Sengupta and Khastgir, 1963; Talapatra et al., 1989, 1998). However, a phytochemical study on the Formosan species has not been reported. As a part of our ongoing investigation and discovery of new anticancer agents, we found that a dichloromethane extract of *G. aequoreum* was active against various human cancer cell lines with $IC_{50} < 20$ μg/ml. Bioactivity-guided chromatographic fractionation of this extract led to the isolation of 17 *ent*-abietane diterpenes, including gelomulides K–X (**1**–**14**), 6β-acetoxy-1-one-8β,14α-dihydroxy-*ent*-abieta-2(3),13(15)-diene-16,12-olide (**15**), gelomulide A (**16**), and gelomulide G (**17**). Gelomulides K–X (**1**–**14**) are new compounds. The structural elucidation of these new diterpenes and the cytotoxic activity of the isolates are reported herein.

2. Results and discussion

The MeOH extract of the dry leaves of *G. aequoreum* was partitioned with CH_2Cl_2 and water (1:1, v/v). Further fractionation of the CH_2Cl_2 extract was carried out by liquid chromatography on silica gel (1000 ml; 63–200 μm) using gradients of CH_2Cl_2–MeOH, which yielded 18 subfractions.

* Corresponding author. Tel.: +886 7 312 1101x2197; fax: +886 7 311 4773.
E-mail address: yachwu@kmu.edu.tw (Y.-C. Wu).

0031-9422/$ - see front matter © 2007 Elsevier Ltd. All rights reserved.
doi:10.1016/j.phytochem.2007.07.005

Chromatographic fractionation of these subfractions led to the isolation of 17 *ent*-abietane diterpenes (Fig. 1).

The HRESIMS of **1** showed an $[M+Na]^+$ ion at *m/z* 395.1835 ($C_{22}H_{28}O_5Na$). The IR spectrum showed absorptions for a α,β-unsaturated γ-lactone carbonyl (1759 cm^{-1}) and an acetate carbonyl (1720 cm^{-1}). Based on the NMR spectroscopic data, compound **1** has a 20-carbon skeleton, an acetoxy group, and an α-methyl α,β-unsaturated γ-lactone [δ_H at 1.95 (*d*, $J = 2.0$ Hz, homoallylic coupling with H-12, Me-17); δ_C 75.7 (C-12), 156.4 (C-13), 128.1 (C-15), 174.0 (C-16), and 8.7 (C-17)], and resembles the reported *Gelonium ent*-abietane diterpenes (Chakravarty et al., 1991; Choudhary et al., 2004; Jahan et al., 2004; Talapatra et al., 1989, 1998). Besides the methyl group on the α,β-unsaturated γ-lactone, three additional methyl groups were also observed. A singlet proton at δ_H 3.94 was attributable to an allylic epoxy proton at C-14. Additional double bond signals (δ_H 5.93 and 5.66, δ_C 119.8 and 143.5) differed from those previously reported for a 1, 2-double bond as found in gelomulide D, gelomulide E, and gelomulide H, or a 2-ene-1-one double bond as observed in 6β-acetoxy-1-one-8β,14α-dihydroxy-*ent*-abieta-2(3),13(15)-diene-16,12-olide, 1-one-8β,14β-epoxy-*ent*-abieta-2(3),13(15)-diene-16,12-olide, and 6β-acetoxy-1-one-8β,14β-epoxy-*ent*-abieta-2(3),13(15)-diene-16,12-olide (Chakravarty et al., 1991; Jahan et al., 2004; Talapatra et al., 1989, 1998). Therefore, 2D NMR spectra were obtained to elucidate fully the structure of **1**. In the HMBC spectrum, the acetoxy methine proton at δ_H 5.28 (*d*, $J = 6$ Hz) exhibited ^2J interactions with C-2 (δ_C 119.8) and C-10 (δ_C 41.9), as well as ^3J interactions with C-3 (δ_C 143.5), C-5 (δ_C 44.8), and C-20 (δ_C 17.8). These and other key HMBC connections are shown in Fig. 2. NOESY correlations were observed between H-5/H-9, H-12/Me-20, and H-12/H-14 (Fig. 3), which indicated the stereochemistry of the chiral centers and ring junctions (*trans* for A/B and *cis* for B/C) in **1**. Thus, compound **1** was elucidated as 1β-acetoxy-8β, 14β-epoxy-*ent*-abieta-2(3),13(15)-diene-16,12-olide and has been named gelomulide K (**1**).

The molecular formula of **2** was deduced as $C_{24}H_{30}O_7$ due to the appearance of an $[M+Na]^+$ ion at *m/z* 453.1887 in the HRESIMS. Furthermore, compounds **1** and **2** have similar spectroscopic data, except that **2** has an additional acetoxy group in comparison with **1**. The NMR spectrum of **2** showed two acetoxy methyls resonating at δ_H 2.05 (*s*, δ_C 21.0) and δ_H 2.10 (*s*, δ_C 21.5), with the corresponding methine signals appearing at δ_H 5.04 (*d*, $J =$ 6.4 Hz, δ_C 71.0) and δ_H 5.06 (*ddd*, $J = 11$, 11, 5.6 Hz, δ_C 70.3), respectively. HMBC correlations (H-1/C-2, C-3, C-10, C-20 and H-6/C-5, C-7) suggested that the acetoxy groups were attached at C-1 and C-6, respectively. The relative stereochemistry of the C-6 acetoxy group was determined to be equatorial based on the multiplicity of the H-6 signal. Both H-1 and H-6 showed NOESY effects with Me-20. This spatial proximity suggested that both acetoxy groups were β-oriented in compound **2**, gelomulide L

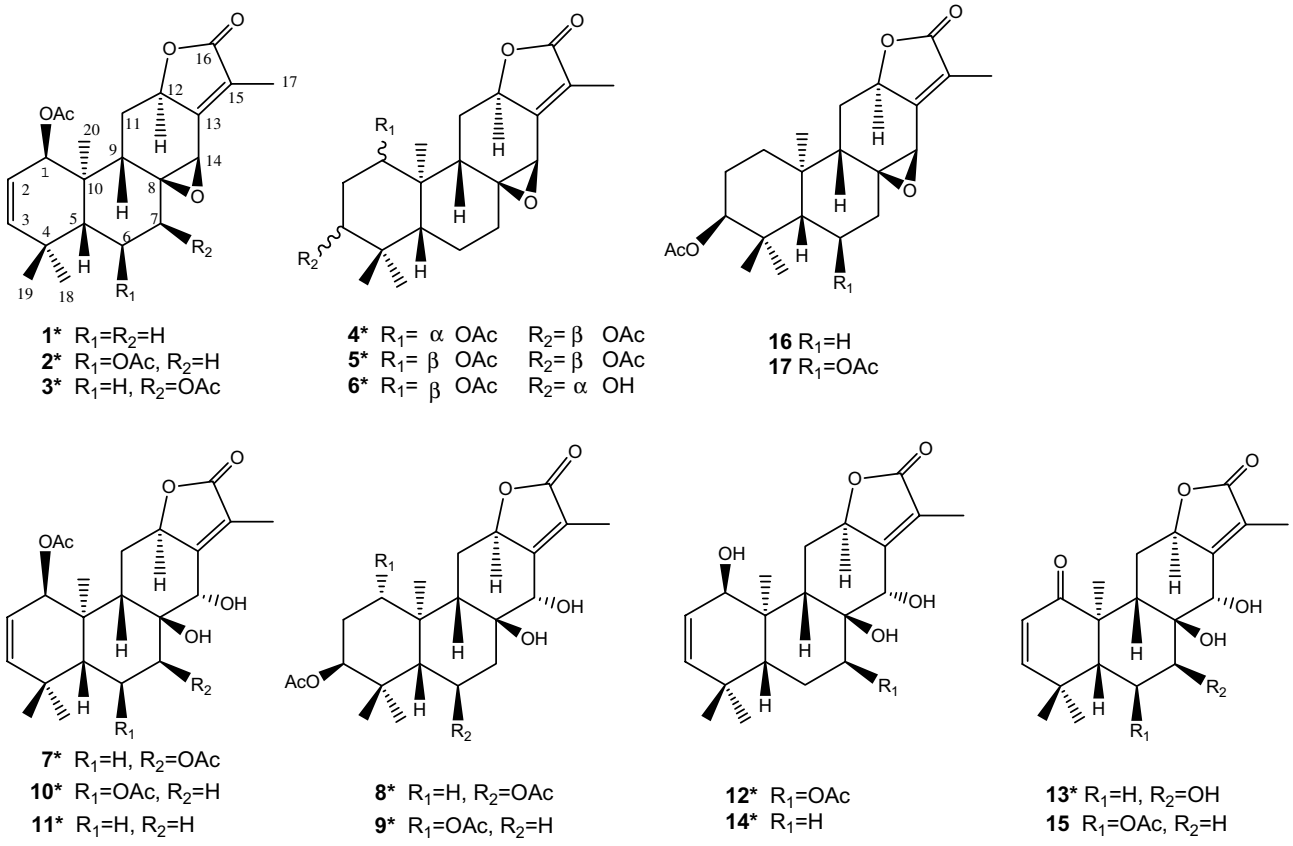

Fig. 1. Structures of compounds **1**–**17**.

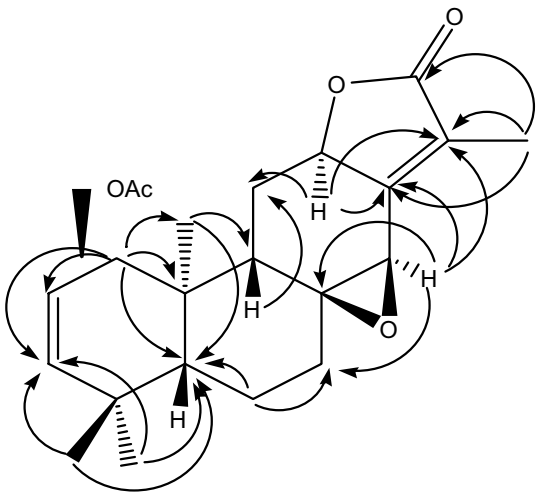

Fig. 2. Important HMBC correlations for compound **1**.

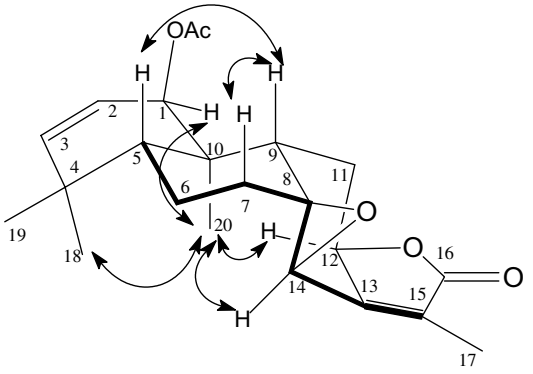

Fig. 3. Important NOESY correlations for compound **1**.

(1β,6β-diacetoxy-8β,14β-epoxy-*ent*-abieta-2(3),13(15)-diene-16,12-olide).

With an $[M+Na]^+$ ion at *m*/*z* 453.1890 in the HRESIMS, compound **3** has the same molecular formula, $C_{24}H_{30}O_7$, as **2**. Likewise, the two compounds have almost identical spectroscopic data, with the only difference between **2** and **3** being the placement of one acetoxy group. In the HMBC spectrum of **3**, the acetoxy methine proton at δ_H 5.22 exhibited a ^2J interaction with C-8 (δ_C 61.4) and a ^3J interactions with C-5 (δ_C 38.2) and C-9 (δ_C 36.1). These correlations led to the assignment of the second acetoxy group at C-7 (δ_C 73.5) rather than C-6 as in **2**. Analysis of coupling constants, together with NOESY correlations between H-7/H-14 and H-6α/Me-20 and no correlation between H-7/H-9, suggested that H-7 is equatorial and α-oriented. The new compound **3** was therefore identified as 1β,7β-diacetoxy-8β,14β-epoxy-*ent*-abieta-2(3),13(15)-diene-16,12-olide, and has been named gelomulide M (**3**).

Compound **4** exhibited an $[M+Na]^+$ ion at *m*/*z* 455.2048 ($C_{24}H_{32}O_7Na$) in the HRESIMS. The molecular formula indicated the absence of the A-ring double bond in comparison with **2** and **3**. However, the NMR signals of the C and D rings were consistent with the NMR spectroscopic data of **1**–**3**. Two acetoxy groups (δ_H 2.06 *s* and 2.15 *s*; δ_C 20.9/170.2 and 21.4/170.0) were also observed in the NMR spectra. From examination of the coupling constants and HMBC spectrum, an axial acetoxy group is present at C-3 [methine proton at δ_H 4.94 (*dd*, $J = 3.6$, 2.4 Hz) with HMBC correlations to C-4 (δ_C 36.7), Me-18 (δ_C 27.9), and Me-19 (δ_C 21.7)], and an equatorial acetate at C-1 [methine proton at δ_H 5.23 (*dd*, $J = 12$, 4.2 Hz) with HMBC correlations to C-2 (δ_C 29.0), C-3 (δ_C 77.9), C-10 (δ_C 43.4) and Me-20 (δ_C 13.6)]. Based on the literature data (Talapatra et al., 1989), H-5, H-9 and Me-20 were assigned as β, β, and α, respectively. Thus, the NOESY correlation between H-1 and H-9 as well as no NOESY correlations between H-1/Me-20, H-3/H-5, or H-1/H-3, indicated β and α orientations for H-1 and H-3, respectively. Thus, the C-1 acetoxy group was α-oriented and the C-3 acetoxy group was β-oriented. The relative stereochemistry of **4** was further confirmed by X-ray crystallographic analysis (Fig. 4), and the structure of **4**, gelomulide N, was elucidated as 1α,3β-diacetoxy-8β,14β-epoxy-*ent*-abieta-13,15-ene-16,12-olide.

Gelomulide O (**5**) was isolated as colorless needles and showed a $[M+Na]^+$ ion at *m*/*z* 455.2047 ($C_{24}H_{32}O_7Na$) in the HRESIMS. The mass and NMR spectroscopic data were similar to those of **4**. On the basis of the HMBC data, the two acetoxy groups were again assigned at C-1 (δ_C 73.5) and C-3 (δ_C 75.7). However, the NOESY correlations of **5** were different from those of **4**, especially those related to H-1. The NOESY correlation observed between H-1 and Me-20 indicated that the C-1 acetate is β- rather than α-oriented. Axial orientations for both acetoxy groups were further supported by the analysis of their coupling constants (H-1, δ_H 5.13, t, $J = 3.2$ Hz; H-3, δ_H 4.90, t, $J = 3.2$ Hz). Thus, compound **5**, 1β,3β-diacetoxy-8β,14β-epoxy-*ent*-abieta-13,15-ene-16,12-olide, is a stereochemical isomer of **4**. Interestingly, compound **5** could be recrystallized from MeOH and separated from its isomer **4**. However, compound **4** and known compound **17**, a positional isomer, had very similar column chromatographic properties, and could be separated only on a recycling HPLC system using a C_{30} reversed phase column.

The molecular formula of **6** is $C_{22}H_{30}O_6$, $[M+Na]^+$ at *m*/*z* 413.1942. The IR spectrum of **6** showed absorptions at 1746 and 3495 cm^{-1}, ascribable to lactone carbonyl and hydroxy functions. The presence of one hydroxy group was inferred from the NMR signal at δ_H 6.14, which was exchangeable with D_2O. Based on the HMBC correlations of H-3 with C-1, C-2, C-18, and C-19, the hydroxy group was assigned at C-3 (δ_C 71.8). In the NOESY spectrum, the correlation between H-1 (δ_H 5.32) and Me-20 (δ_H 1.13) as well as the correlation between H-3 (δ_H 4.00) and H-5 (δ_H 1.63) suggested the following orientations, β-OAc and α-OH. Therefore, new compound **6** was identified as 1β-acetoxy-3α-hydroxy-8β,14β-epoxy-*ent*-abieta-13,15-ene-16,12-olide, and has been named gelomulide P.

In the ^1H NMR spectra, compounds **7**–**15** showed a downfield-shifted singlet at δ_H 4.6–5.1 in place of the allylic

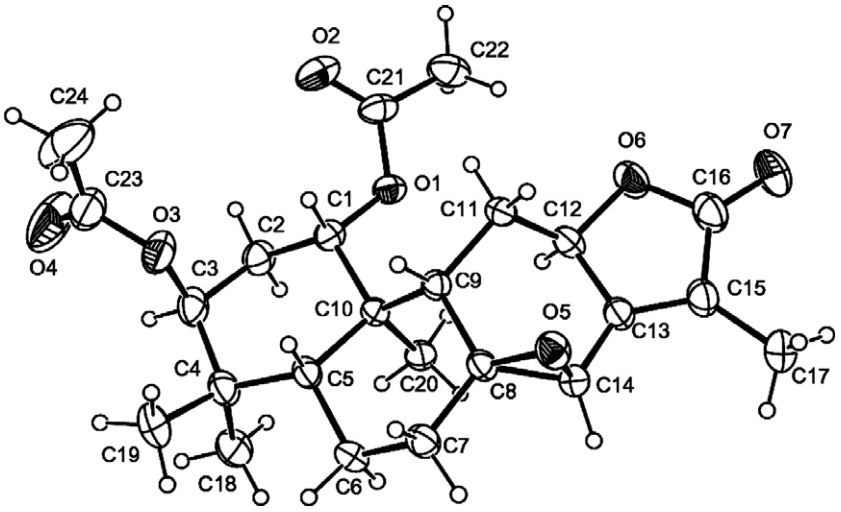

Fig. 4. X-ray crystal structure of compound **4**.

epoxy proton singlet (H-14) at δ_H 3.8–4.3 found in **1**–**6**, **16**, and **17**. In addition, in the ^{13}C NMR spectra, C-14 was found at δ_C 71–74 in **7**–**15** rather than δ 55–56, and C-8 was found at δ 74–76 rather than δ 60-61. Based on these data, compounds **7**–**15** are 8,14-dihydroxyl *ent*-abietane diterpenes (Choudhary et al., 2004; Talapatra et al., 1998).

The HRESIMS of **7** showed an $[M+Na]^+$ ion at *m*/*z* 471.1995 ($C_{24}H_{32}O_8Na$) while FABMS gave an $[M+H]^+$ ion at *m*/*z* 449 with sequential losses of two acetic acid units resulting in fragment ions at *m*/*z* 389 ($[M+H]^+$-AcOH) and 329 (389-AcOH). Two acetoxy methine protons appeared in the ^1H NMR spectrum at δ_H 5.01 and 5.17. The HMBC correlations of H-1 (δ_H 5.01) with C-2, C-3, C-5, C-10, C-20 and of H-7 (δ_H 5.17) with C-5, C-8, C-9 suggested that the two acetoxy groups were at C-1 and C-7, respectively. In the 1D NMR spectrum, intra-ring olefinic proton resonances were found at δ_H 5.75 and 5.66 as doublets ($J = 10$ Hz) with their carbons appearing at δ_C 119.7 and 142.9, respectively. These substitutions were similar to those of **3**. The 8,14-dihydroxyl substitutions were confirmed by NMR signals for C-8 at δ_C 74.3 and C-14 at δ_C 70.6 (Choudhary et al., 2004; Talapatra et al., 1998). Together with the related coupling constants between H-5, H-6, and H-7 (Table 3), the presence of NOESY correlations (Fig. 5) established that not only is H-7 equatorial and α-oriented, but the C-8 and C-14 hydroxyls are β- and α-oriented, respectively. From these data, new compound **7** was elucidated as 1β,7β-diacetoxy-8β,14α-dihydroxy-*ent*-abieta-2(3),13(15)-diene-16,12-olide and has been named gelomulide Q (**7**).

The IR spectrum of compound **8** showed absorptions for hydroxy (3446 cm^{-1}), α,β-unsaturated γ-lactone carbonyl (1734 cm^{-1}), and acetate carbonyl (1733 cm^{-1}) groups. The HRESIMS of **8** showed a $[M+Na]^+$ ion at *m*/*z* 473.2149 ($C_{24}H_{34}O_8Na$). By comparing the 1D NMR spectra of **8** and gelomulide G (**17**), the new compound **8** was found to be the 8,14-dihydroxy analog of **17** with the following consistent changes in the NMR chemical shifts:

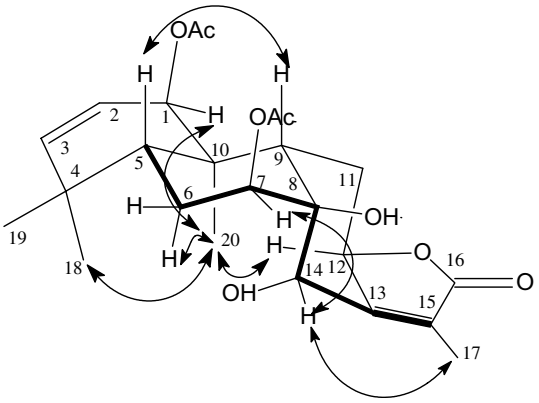

Fig. 5. Important NOESY interactions for compound **7**.

H-14 appeared at δ_H 4.92 in **8** rather than at δ_H 3.85 for the typical epoxy proton resonance in **17**, and the C-8 and C-14 ^{13}C NMR signals were shifted to δ_C 76.0 and 72.3 in **8** from ca. δ_C 60 and 56, respectively, in the 8,14-epoxy analogs. Thus, compound **8** was elucidated as 3β,6β-diacetoxy-8β,14α-dihydroxy-*ent*-abieta-13,15-ene-16,12-olide and was given the name gelomulide R (**8**).

Likewise, compounds **9**–**11** were found to be the 8,14-dihydroxy derivatives of gelomulides N (**4**), L (**2**), and K (**1**), and have been named gelomulides S–U, respectively. The NMR assignments are detailed in Tables 3 and 4.

The HRESIMS of gelomulide V (**12**) afforded an $[M+Na]^+$ ion at *m*/*z* 429.1891 ($C_{22}H_{30}O_7Na$), and the IR spectrum showed absorptions for hydroxy (3289 cm^{-1}), α,β-unsaturated γ-lactone carbonyl (1720 cm^{-1}), and acetoxy carbonyl (1718 cm^{-1}) groups. The NMR spectra showed a carbinol proton at δ_H 4.10 (*d*, $J = 5.6$ Hz) with the corresponding carbon at δ_C 69.5, as well as an acetoxy methyl resonance at δ 1.89 (*s*, δ_C 21.1) with the corresponding methine signal at δ_H 5.89 (*t*, $J = 2$ Hz, δ_C 76.5). The HMBC correlations of H-1 (δ_H 4.1) with C-2 (δ_C 125.7), C-3 (δ_C 139.8), C-5 (δ_C 36.9), C-10 (δ_C 42.8), and C-20

(δ_C 18.3) and of H-7 (δ_H 5.89) with C-5 (δ_C 36.9), C-8 (δ_C 74.8), C-9 (δ_C 43.0), C-14 (δ_C 70.8), and O*C*OMe (δ_C 170.3) suggested that the hydroxy group was positioned at C-1 and the acetoxy group at C-7. Gelomulide V (**12**) was elucidated as 7β-acetoxy-1β-hydroxy-8β,14α-dihydroxy-*ent*-abieta-2(3),13(15)-diene-16,12-olide. To determine the absolute configuration, we treated compound **12** separately with (*R*)- and (*S*)-α-methoxy-α-(trifluoromethyl)-phenylacetyl chloride [(*R*)- and (*S*)-MTPA-Cl] in the presence of pyridine-d_5 to yield the (*S*)- and (*R*)-MTPA esters (**12a** and **12b**), respectively. The MTPA esters were generated successfully at both C-1 and C-14, as elucidated from the ^{1}H NMR spectra (**12a**, H-1, δ_H 5.53, *d*, $J = 6.0$ Hz; H-14, δ_H 5.11, *s*; **12b**, H-1, δ_H 5.49, *d*, $J = 6.0$ Hz; H-14, δ_H 5.15, *s*). The differences between the ^{1}H NMR chemical shifts for **12a** and **12b** (Δ values shown in Fig. 6) led to the assignments of the *S*-configuration at C-1 and *R*-configuration at C-14.

Compound **13** has the molecular formula $C_{20}H_{26}O_6$ as established by HRESIMS (*m*/*z* 385.1625 $[M+Na]^+$). Its IR spectrum showed absorptions attributable to hydroxy (3326 cm^{-1}), α,β-unsaturated γ-lactone carbonyl (1738 cm^{-1}), and α,β-unsaturated carbonyl (1666 cm^{-1}) groups. In the NMR spectra, the presence of two conjugated carbonyls was apparent from the appearance of intra-ring coupled olefinic proton resonances at δ_H 5.92 and 6.35 (each 1H, *d*, $J = 10$ Hz) and carbon signals at δ_C 124.4, 155.7, and 206.3, in addition to the characteristic signals for an α,β-unsaturated γ-lactone as in prior reported compounds. According to the HMBC correlations (H-2/C-4, C-10, H-3/C-1, C-4, C-18, C-19, and H-20/C-1), the additional double bond was at C-2 and C-3 and the carbonyl group at C-1. The proton at δ_H 4.47 exhibited a ^2J interaction with C-6 (δ_C 29.1) and ^3J interaction with C-5 (δ_C 41.1), leading to the assignment of the hydroxy group at C-7. New compound **13** (7β-hydroxy-1-one-8β,14α-dihydroxy-*ent*-abieta-2(3),13(15)-diene-16,12-olide) has been named gelomulide W (**13**).

The molecular formula of gelomulide X (**14**) was determined to be $C_{20}H_{28}O_5$ on the basis of HRESIMS (*m*/*z* 371.1832 $[M+Na]^+$). The presence of the hydroxy groups and a lactone moiety were indicated from the IR spectrum (3406 and 1737 cm^{-1}). The NMR spectroscopic data were similar to those of compound **12**, but no acetoxy signal was observed. The HMBC correlations of H-1 (δ_H 4.12) with C-2 (δ_C 125.7), C-3 (δ_C 139.9), C-5 (δ_C 44.8), C-10 (δ_C 43.0), and C-20 (δ_C 18.6) suggested that the hydroxy group is positioned at C-1. In order to determine the absolute configuration, we treated compound **14** with both (*R*)- and (*S*)-MTPA-Cl in the presence of pyridine-d_5 to yield the (*S*)- and (*R*)-MTPA esters (**14a** and **14b**), respectively. Comparison of the ^{1}H NMR chemical shifts for **14a** and **14b** (Δ values in Fig. 6) led to the assignment of the *S*- and *R*-configuration at C-1 and C-14, respectively, as also found in **12**.

The IR spectrum of compound **15** showed absorptions for hydroxy (3475 cm^{-1}), α,β-unsaturated carbonyl (1748 cm^{-1}), acetate carbonyl (1731 cm^{-1}), and α,β-unsaturated carbonyl (1684 cm^{-1}) groups. The NMR spectroscopic data were similar to those of **13**. The ^{1}H NMR spectrum showed signals for an acetoxy methine proton at δ_H 6.23 (*ddd*, $J = 11.6$, 11.1, 4 Hz) and acetoxy methyl protons at δ_H 2.09. The intra-ring double bond [δ_H 5.93 and 6.24 ($J = 10$ Hz), δ_C 122.9 and 156.3] was also deduced from the ^{1}H NMR spectrum. The HMBC correlation of Me-20 (δ_H 1.82) with C-1 (δ_C 204.8) was interpreted

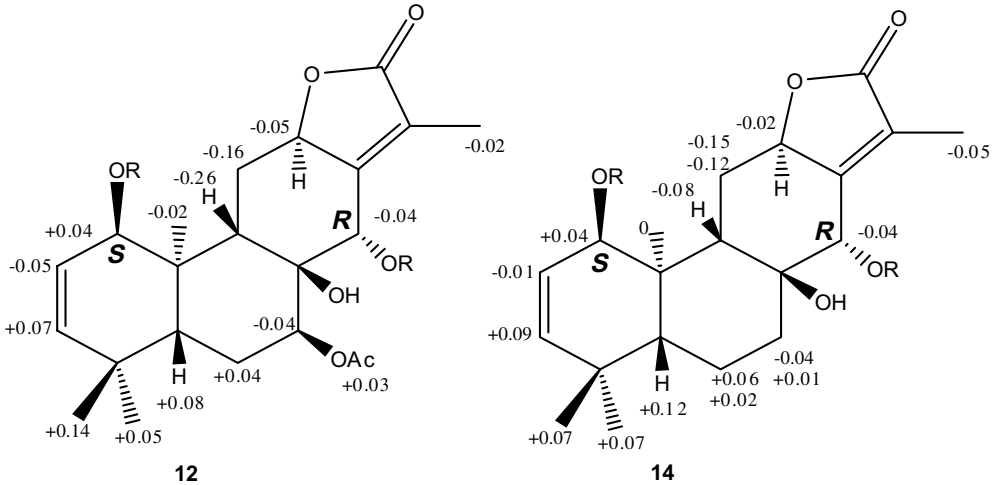

Fig. 6. ^{1}H NMR chemical shift differences [δ(*S*)-MTPA − δ(*R*)-MTPA] of the MTPA esters.

to mean that the carbonyl group was at C-1. The structure was elucidated as 6β-acetoxy-1-one-8β,14α-dihydroxy-*ent*-abieta-2(3),13(15)-diene-16,12-olide. Although this compound was reported earlier by Choudhary et al. (2004), our data differed somewhat from the earlier literature values (Choudhary et al., 2004). Firstly, compound **15** did not dissolve well in $CHCl_3$, while the earlier reported compound did. Secondly, C-13 and C-15 of **15** appeared at δ_C 164.2 and 121.8, but were earlier reported at δ_C 156.1 and 128.0. Thirdly, our compound **15** had a negative optical rotation in contrast with the positive rotation of the earlier reported structure. Based on these differences and particularly the ^{13}C NMR spectroscopic data, we believe that the previously reported compound has a 8,14-epoxy function as found in **1**–**6**, **16**, and **17** (Table 2).

Compounds **16** and **17** differed only by the presence of a 6β-acetoxy group at C-7 consistent with the difference in the molecular formula ($C_{22}H_{30}O_5$, *m*/*z* 374.2170 for **16**; $C_{24}H_{32}O_7$ *m*/*z* 432.2049 for **17**) in HRESIMS. By comparing the spectroscopic (Tables 1 and 2) and physical data of **16** and **17** with the literature values, we found these compounds to be the known gelomulide A and gelomulide G (Choudhary et al., 2004; Talapatra et al., 1998).

Generally, the ^1H NMR spectra of all compounds showed a characteristic doublet for the lactone Me-17, which resonated at ca. δ_H 1.80–1.98 (δ_C 8.5–8.8) with a coupling constant of ca. 1.6–2.4 Hz, and the CD spectra of **1**–**17** showed a positive Cotton effect at ca. 250 nm ($n \rightarrow \pi^*$) and a negative effect at ca. 215 nm ($\pi \rightarrow \pi^*$). These data suggested that the α,β-unsaturated γ-lactone chromophore has left-handed chirality (*R*-form at C-12) (Beecham, 1972; Chakravarty et al., 1991).

Compounds **1**–**17** were screened in an *in vitro* cytotoxicity assay. Gelomulide K (**1**) and gelomulide M (**3**) showed moderate cytotoxic activity against lung (A549), breast (MEA-MB-231 and MCF7), and liver (HepG2) cancer cell lines. Doxorubicin was used as a positive control, and the data shown in Table 5. While only **1** and **3** showed activity, **1** is the major component of this plant, and is possibly the major active principle of the crude extract. In previous studies on the cytotoxicity of *Gelonium ent*-abietane diterpenes, only one compound, 6β-acetoxy-1-one-8β,14α-dihy-

Table 1
^1H NMR spectroscopic data of compounds **1**–**6** and **16**–**17** (**2** and **16** in $CDCl_3$; **1**, **3**–**6**, and **17** in C_5D_5N); δ in ppm, *J* in Hz

Protons	1	2	3	4	5	6	16	17
1	5.28 *d*(6)	5.04 *d*(6.4)	5.35 *d*(6)	5.23 *dd*(12,4.2)	5.13 *t*(3.2)	5.32 *t*(2)	a −1.53 *m* b −1.73 *m*	α −1.48 *m* β −1.45 *m*
2	5.93 *dd* (10, 6)	5.81 *dd* (9.6, 6.4)	5.96 *dd* (10, 6)	α −1.88 *ddd* (14.4, 12, 2.4) β −1.58 *ddd* (14.4, 4.2, 3.6)	α −2.11 *dt* (16, 3.2) β −2.38 *dt* (16, 3.2)	α −2.12 *ddd* (14.2, 12.8, 2) β −2.34 *ddd* (14.2, 4.2, 2)	a −1.76 *m* b −1.88 *m*	α −1.71 *m* β −1.77 *m*
3	5.66 *d* (10)	5.62 *d* (9.6)	5.69 *d* (10)	4.94 *dd* (3.6, 2.4)	4.90 *t* (3.2)	4.00 *dt* (12.8)	4.71 *t* (2.8)	4.80 *t* (2.8)
5	1.80 *dd* (12.8, 2.8)	2.11 *d* (11)	2.38 *dd* (13.6, 2.8)	1.63 *m*	1.92 *dd* (12.8, 2.4)	1.63 *dd* (12.4)	1.48 *m*	1.87 *d* (11.6)
6	α −1.48 *ddd* (14, 12.8, 4) β −1.64 *m*	5.06 *ddd* (11, 11, 5.6)	α −1.83 *ddd* (14.4, 13.6, 2.8) β −2.07 *ddd* (14.4, 2.8, 2.8)	a −1.57 *m* b −1.58 *m*	α −1.48 *m* β −1.64 *m*	α −1.75 *m* β −1.56 *dt* (13, 3.4)	a −1.49 *m* b −1.70 *m*	5.38 *ddd* (13.4, 11.6, 5.8)
7	α −1.66 *m* β −1.99 *m*	a −2.03 *m* b −2.06 *m*	5.22 *t* (2.8)	a −1.65 *dt* (13.6, 3.4) b −1.98 *m*	α −1.67 *m* β −1.99 *ddd* (14.4, 14.4, 6)	α −1.69 *ddd* (13.6, 3.2, 3.2) β −1.99 *m*	a −1.67 *m* b −2.02 *m*	α −2.13 *dd* (13.4, 5.8) β −2.09 *dd* (13.4, 13.4)
9	2.76 *d* (7.2)	2.56 *d* (6.8)	3.22 *d* (7.2)	2.14 *d* (6.8)	2.76 *d* (7.2)	2.62 *d* (6.8)	2.08 *d* (6.8)	1.99 *d* (6.8)
11	α −2.30 *dd* (13.4, 5.6) β −1.55 *ddd* (13.4, 13.2, 7.2)	α −2.11 *dd* (13.6, 5.4) β −1.42 *ddd* (13.6, 13.3, 6.8)	α −2.39 *dd* (13.6, 6) β −1.58 *ddd* (13.6, 13.3, 7.2)	α −2.39 *dd* (13.6, 5.2) β −1.59 *ddd* (13.6, 13.3, 6.8)	α −2.17 *dd* (13.2, 6) β −1.49 *ddd* (13.2, 13.2, 7.2)	α −2.25 *dd* (13.6, 5.6) β −1.49 *ddd* (13.6, 13.2, 6.8)	α −2.29 *dd* (13.4, 5.6) β −1.42 *ddd* (13.4, 13.2, 6.8)	α −2.30 *dd* (13.2, 5.6) β −1.45 *ddd* (13.2, 13.2, 6.8)
12	5.13 *ddd* (13.2, 5.6, 2)	4.92 *ddd* (13.3, 5.4, 2.4)	5.22 *ddd* (13.3, 6, 2.4)	5.22 *ddd* (13.3, 5.2, 2)	5.12 *ddd* (13.2, 6, 2.4)	5.13 *ddd* (13.2, 5.6, 2)	5.00 *ddd* (13.2, 5.6, 2.4)	5.05 *ddd* (13.2, 5.6, 2)
14	3.94 *s*	3.93 *s*	4.33 *s*	3.91 *s*	3.93 *s*	3.92 *s*	3.77 *s*	3.85 *s*
17	1.95 *d* (2)	1.98 *d* (2.4)	1.95 *d* (2.4)	1.95 *d* (2)	1.95 *d* (2.4)	1.94 *d* (2)	1.97 *d* (2.4)	1.97 *d* (2)
18	0.89 *s*	1.01 *s*	0.88 *s*	0.89 *s*	0.90 *s*	1.12 *s*	0.99 *s*	0.98 *s*
19	1.00 *s*	1.23 *s*	1.01 *s*	0.91 *s*	0.98 *s*	1.30 *s*	0.92 *s*	1.18 *s*
20	1.01 *s*	1.05 *s*	1.08 *s*	1.25 *s*	1.08 *s*	1.13 *s*	1.10 *s*	1.07 *s*
COO*Me*	C1–COO*Me* 1.98 *s*	C1–COO*Me* 2.05 *s* C6–COO*Me* 2.10 *s*	C1–COO*Me* 1.97 *s* C7–COO*Me* 2.10 *s*	C1–COO*Me* 2.15 *s* C3–COO*Me* 2.06 *s*	C1–COO*Me* 2.09 *s* C3–COO*Me* 2.11 *s*	C1–COO*Me* 1.99 *s*	C3–COO*Me* 2.08 *s*	C3–COO*Me* 2.20 *s* C6–COO*Me* 2.07 *s*

Table 2
^{13}C NMR spectroscopic data of compounds **1**–**6** and **16**–**17** (**2** and **16** in $CDCl_3$; **1**, **3**–**6**, and **17** in C_5D_5N); δ in ppm

Carbons	1	2	3	4	5	6	16	17
1	71.3	71.0	71.2	76.1	73.5	75.8	33.8	33.5
2	119.8	118.0	119.9	29.0	25.8	31.9	22.6	22.5
3	143.5	144.7	143.3	77.9	75.7	71.8	77.1	78.8
4	35.1	35.3	34.7	36.7	36.6	39.4	36.7	36.8
5	44.8	47.7	38.2	49.3	43.9	48.8	48.7	52.2
6	21.5	70.3	27.2	20.5	20.5	20.8	20.4	69.6
7	34.4	39.3	73.5	33.9	34.3	34.6	34.6	40.3
8	61.4	59.6	61.4	61.3	61.4	61.4	60.9	59.7
9	39.8	39.2	36.1	48.9	41.8	42.1	49.0	48.1
10	41.9	41.4	41.7	43.4	42.3	42.4	38.9	39.1
11	24.0	23.5	23.9	26.7	23.8	23.9	23.8	24.3
12	75.7	75.0	75.5	75.3	75.5	75.5	75.5	75.4
13	156.4	154.2	154.7	156.5	156.4	156.4	155.5	156.0
14	55.8	55.6	55.1	55.8	56.0	56.0	56.1	55.7
15	128.1	129.5	129.0	128.9	128.4	128.4	128.8	128.8
16	174.0	173.5	173.6	173.9	173.9	173.9	173.9	173.9
17	8.7	8.8	8.7	8.8	8.7	8.7	8.8	8.8
18	23.6	23.3	23.3	27.9	22.5	16.6	22.2	22.3
19	31.6	33.8	31.2	21.7	28.2	29.3	28.4	31.6
20	17.8	18.9	17.5	13.6	18.2	18.5	19.2	19.9
COO*Me*	20.8	21.0, 21.5	20.8, 21.0	20.9, 21.4	21.0, 21.1	20.8	21.2	21.0, 21.6
*C*OOMe	170.1	170.0, 170.0	170.1, 170.0	170.2, 170.0	170.0, 170.2	170.0	170.5	170.2, 170.1

droxy-*ent*-abieta-2(3),13(15)-diene-16,12-olide, showed promising activity against the NCI-H460 (Lung) cell line with a growth inhibition of over 85% at concentration of 50 μM (Choudhary et al., 2004). In comparison with the data, we speculated that 8,14-epoxy and 2,3-double bond moieties might be necessary for a cytotoxic activity.

2.1. Concluding remarks

In this genus, the main structural skeleton, *ent*-abietane-type diterpene, has been reported in past studies (Chakravarty et al., 1991; Choudhary et al., 2004; Das and Chakravarty, 1993; Jahan et al., 2002, 2004; Parveen and Khan, 1987; Talapatra et al., 1989, 1998). However, the 14 new compounds, gelomulides K–X (**1**–**14**), isolated and characterized in this study illustrate the interesting biodiversity and novelty of this aboriginal plant. The structures of most of the new compounds are different from those found in prior studies (Chakravarty et al., 1991; Choudhary et al., 2004; Das and Chakravarty, 1993; Jahan et al., 2002, 2004; Parveen and Khan, 1987; Talapatra et al., 1989, 1998). For instance, the previously known compounds seldom had a double bond at C-2 and C-3, and when such a double bond was occasionally found, it was always accompanied by a carbonyl group at C-1, forming a 2-en-1-one functionality. In this plant, different oxygenated substituents (ketone, hydroxyl, acetate) were found at C-1 while the 2,3-double bond was present. Furthermore, the isolates displayed different permutation and combinations of the oxygenated substituents at C-1, C-3, C-6, C-7, C-8, or C-14 when the 2,3-double bond function was absent. Also, based on the NMR spectroscopic data in the current study, two major classes of *ent*-abietanes, 8,14-epoxy (**1**–**6** and **16**–**17**) and 8,14-dihydroxy (**7**–**15**) analogs, can be elucidated easily from *Gelonium* species. During the extraction, partition, and isolation procedures, acidic or alkaline reagents, such as acetic acid, NH_4OH aq, etc., were not applied. Compounds possessing acetoxy groups or diol should not be artifacts.

The diterpenes are C_{20} compounds biogenetically derived from geranylgeranyl pyrophosphate. A notable feature of diterpene structures is the fascinating variation encountered in their skeletons, and the occurrence in nature of both normal and antipodal (enantio- or ent-) stereochemical series (Devon and Scott, 1972; Nakanishi et al., 1974). Most abietane diterpenes should belong to the normal absolute configuration, as according to the research and classifications of Devon and Nakanishi et al., only kaurane-type skeletons occur exclusively or almost exclusively in the antipodal forms in nature. Therefore, the absolute configuration assignments herein of *Gelonium* *ent*-abietane diterpenes, which depend critically on the validity of the CD correlations, seem to be rare exceptions (Chakravarty et al., 1991; Choudhary et al., 2004; Jahan et al., 2004; Talapatra et al., 1989, 1998).

3. Experimental

3.1. General experimental procedures

Melting points were determined on a Fisher-Johns Melting Point apparatus. UV spectra were measured on a Jasco V-530 UV/VIS spectrophotometer. IR spectra were recorded on a Mattson Genesis II™ FT-IR spectrophotometer. The optical rotations were taken on a Jasco-P-1020

Table 3
^{1}H NMR spectroscopic data of compounds **7**–**15** (**7** in $CDCl_3$; **8**–**15** in C_5D_5N); δ in ppm, J in Hz

Protons	**7**	**8**	**9**	**10**	**11**	**12**	**13**	**14**	**15**
1	5.01 *d* (6)	α −1.60 *ddd* (12.8, 3.4, 3.4) β −1.40 *ddd* (13.3, 12.8, 3.4)	5.35 *dd* (10.8, 5.2)	5.35 *d* (6.3)	5.33 *d* (6)	4.10 *d* (5.6)		4.12 *d* (6)	
2	5.75 *dd* (10, 6)	α −1.89 *m* β −1.71 *dq* (14.8, 3.4)		5.96 *dd* (10, 6.3)	5.93 *dd* (10, 6)	6.08 *dd* (10, 5.6)	5.92 *d* (10)	6.08 *dd* (10, 6)	5.93 *d* (10)
3	5.66 *d* (10)	4.83 *t* (2.6)	4.96 *t* (3.2)	5.61 *d* (10)	5.60 *d* (10)	5.60 *d* (10)	6.35 *d* (10)	5.60 *d* (10)	6.24 *d* (10) 2.18 *d* (11.1)
5	1.96 *dd* (13.6, 2.4)	2.19 *d* (11.2)	1.95 *dd* (13, 2.8)	2.39 *d* (11.6)	1.92 *dd* (12.8, 3)	2.51 *dd* (13.2, 2)	2.67 *d* (13, 2.8)	2.07 *dd* (12.8, 3)	
6	α −2.22 *ddd* (14, 13.6, 2.8) β −1.91 *ddd* (14, 2.4, 2.8)	5.97 *ddd* (11.2, 9, 4.6)	a −1.71 *m* b −2.22 *m*	6.08 *ddd* (11.8, 11.6, 4.6)	α −1.73 *m* β −2.38 *dddd* (13.2, 13.2, 13.2, 3)	α −2.79 *ddd* (14, 13.2, 2) β −2.14 *ddd* (14, 2, 2)	α −2.91 *ddd* (13.3, 13.3, 2.2) β −2.13 *ddd* (13.2, 2.8, 2.2)	α −1.75 *m* β −2.49 *dddd*	6.23 *ddd* (11.6, 11.1, 4) (12.8, 12.8, 12.8, 3)
7	5.17 *t* (2.8)	α −2.27 *dd* (13, 9) β −3.02 *dd* (13, 4.6)	a −2.09 *m* b −2.67 *m*	α −3.09 *dd* (12.4, 4.6) β −2.26 *dd* (12.4, 11.8)	α −2.11 *m* β −2.69 *ddd* (13.2, 3, 3)	5.89 *t* (2)	4.47 *t* (2.2)	α −2.15 *ddd* (13.5, 13.5, 3.8) β −2.72 *ddd* (13.2, 3, 3)	α −2.98 *dd* (12.4, 4) β −2.17 *dd* (12.4, 11.6)
9	2.28 *d* (8)	2.08 *d* (7.6)	2.33 *d* (6.8)	2.78 *d* (7.6)	2.75 *d* (8)	3.7 *d* (7.6)	3.06 *d* (7.6)	3.46 *d* (7.6)	2.95 *d* (7.8)
11	α −2.27 *m* β −1.56 *ddd* (12.6, 12.6, 8)	α −2.65 *dd* (10.2, 6.6) β −2.09 *m*	α −3.03 *dd* (15.6, 6.4) β −2.32 *m*	α −2.70 *dd* (13.6, 6.8) β −2.13 *ddd* (13.6, 12.2, 7.6)	α −2.63 *dd* (13.2, 6.8) β −2.13 *m*	α −2.83 *dd* (12.8, 6.8) β −2.22 *ddd* (12.8, 12.8, 7.6)	α −3.45 *dd* (13.6, 6.8) β −2.49 *ddd* (13.6, 12.6, 7.6)	α −2.87 *dd* (13, 6.8) β −2.32 *ddd* (13, 12.5, 7.6)	α −3.18 *dd* (13.8, 7.2) β −2.50 *ddd* (13.8, 13.3, 7.8)
12	5.21 *m*	5.56 *m*	5.71 *m*	5.57 *ddd* (12.2, 6.8, 2)	5.61 *ddd* (13.2, 6.8, 2)	5.75 *ddd* (12.8, 6.8, 2)	5.65 *ddd* (12.6, 6.8, 1.6)	5.74 *ddd* (12.5, 6.8, 1.6)	5.51 *ddd* (13.3, 7.2, 1.6)
14	4.64 *s*	4.92 *s*	4.96 *s*	4.97 *s*	5.02 *s*	5.12 *s*	5.01 *s*	5.08 *s*	4.97 *s*
17	1.86 *d* (2)	1.89 *d* (2)	1.85 *d* (1.6)	1.84 *d* (2)	1.83 *d* (2)	1.80 *d* (2)	1.82 *d* (1.6)	1.86 *d* (1.6)	1.85 *d* (1.6)
18	0.91 *s*	1.05 *s*	0.96 *s*	1.07 *s*	0.93 *s*	0.96 *s*	1.08 *s*	1.00 *s*	1.15 *s*
19	0.97 *s*	1.21 *s*	0.92 *s*	1.34 *s*	1.04 *s*	0.96 *s*	1.03 *s*	1.02 *s*	1.26 *s*
20	1.25 *s*	1.47 *s*	1.67 *s*	1.59 *s*	1.52 *s*	1.56 *s*	1.79 *s*	1.57 *s*	1.82 *s*
COO*Me*	C1–COO*Me* 2.04 *s* C7–COO*Me* 2.15 *s*	C3–COO*Me* 2.09 *s* C6–COO*Me* 2.01 *s*	C1–COO*Me* 2.08 *s* C3–COO*Me* 1.99 *s*	C1–COO*Me* 1.84 *s* C6–COO*Me* 2.12 *s*	C1–COO*Me* 1.82 *s*	C7–COO*Me* 1.89 *s*			C6–COO*Me* 2.09 *s*

Table 4
^{13}C NMR spectroscopic data of compounds **7**–**15** (**7** in $CDCl_3$; **8**–**15** in C_5D_5N); δ in ppm

Carbons	7	8	9	10	11	12	13	14	15
1	71.5	35.5	79.9	72.1	72.2	69.5	206.3	69.5	204.8
2	119.7	23.1	29.8	119.2	120.4	125.7	124.4	125.7	122.9
3	142.9	79.5	78.3	144.8	143.4	139.8	155.7	139.9	156.3
4	34.6	37.0	36.9	35.7	35.3	34.9	36.2	35.4	36.9
5	37.1	52.3	43.3	48.8	45.8	36.9	41.1	44.8	52.7
6	26.4	70.8	20.0	72.0	22.0	27.6	29.1	22.2	71.2
7	75.7	47.3	39.9	48.0	42.3	76.5	72.3	42.7	47.9
8	74.3	76.0	75.7	75.4	74.6	74.8	76.1	74.9	75.3
9	43.2	56.1	55.8	46.0	46.5	43.0	43.9	46.0	46.4
10	40.8	39.2	43.3	42.1	41.7	42.8	49.3	43.0	49.7
11	28.4	29.2	31.3	29.3	29.6	29.4	32.8	29.9	32.4
12	76.5	77.7	77.8	77.2	77.4	77.8	78.0	78.0	77.6
13	159.8	164.3	164.5	164.2	164.7	164.2	164.2	165.4	164.2
14	70.6	72.3	73.9	71.6	73.0	70.8	70.9	73.2	72.0
15	124.2	122.2	121.7	122.3	121.8	122.3	121.5	121.5	121.8
16	174.5	175.1	175.2	175.0	175.1	175.1	175.1	175.3	175.1
17	8.5	8.7	8.6	8.5	8.5	8.5	8.5	8.5	8.5
18	22.2	22.5	21.9	22.6	22.8	22.6	21.8	23.0	21.8
19	31.0	31.7	28.1	34.1	31.6	31.0	30.9	31.6	34.0
20	17.6	18.3	12.7	18.6	18.1	18.3	17.8	18.6	19.0
COO*Me*	21.2, 21.2	21.0, 21.8	21.5, 20.8	20.7, 21.7	20.8	21.1			21.6
*C*OOMe	170.2, 170.7	170.2, 170.1	170.2, 170.2	170.1, 170.1	170.1	170.3			170.0

Table 5
Cytotoxicity of compounds **1** and **3**

Compound	(IC_{50}: μM)/cell line			
	A549	MDA-MB-231	MCF7	HepG2
Gelomulide K (**1**)	25.0 ± 0.13	26.5 ± 0.02	29.8 ± 0.16	21.4 ± 0.14
Gelomulide M (**3**)	14.6 ± 0.01	15.1 ± 0.56	15.0 ± 0.12	10.5 ± 0.08
Doxorubicin	0.83 ± 0.02	0.72 ± 0.00	0.66 ± 0.01	0.86 ± 0.00

Compounds were tested as a maximum concentration of 50 μM. Results are the mean ± SD.

polarimeter (cell length 10 mm). Circular dichroism spectra were measured on a Jasco J-810 spectrophotometer. The NMR spectra were recorded on Varian Unity-plus 400 MHz FT-NMR and Varian Mercury-plus 400 MHz FT-NMR instruments. The chemical shift (δ) values are in ppm (part per million) with $CDCl_3$ and C_5D_5N as internal standard, and coupling constants (J) are in Hz. HRESI-MS and FAB-MS measurement were performed on a Bruker Daltonics APEX II 30e mass spectrometer and VG Biotech Quattro 5022 mass spectrometer, respectively. TLC was performed on Kieselgel 60, F 254 (0.20 nm, Merck), spots were viewed under ultraviolet light at 254 nm and 356 nm and/or stained by spraying with 50% H_2SO_4 and heating on a hot plate. For column chromatography, silica gel (Kiesilgel 60, 70–230, and 230–400 mesh, Merck) and Sephadex LH-20 were used. Further purification of some compounds was achieved by preparative HPLC, Shimadzu LC-10AT and recycling HPLC, LC-918 (JAI) and Discovery column (250×10 mm, C_{18}), Hypersil ODS column (250×21.2 mm, C_{18}), and Develosil™ column (250×21.2 mm, C_{30}) were used. For Mosher's ester derivatives, (*S*)-(+)- and (*R*)-(−)-α-methoxy-α-(trifluoromethyl)-phenylacetyl chloride were used as the reagents.

3.2. Plant material

The plant material (440 g) was collected in Taichung County, Taiwan, in April, 2004. The plant was identified by Dr. Hsin-Fu Yen of the National Museum of Natural Science, Taichung, Taiwan.

3.3. Extraction and isolation

The dry leaves of *G. aequoreum* (440 g) were extracted three times with MeOH at room temperature to obtain a crude extract (68.5 g). The crude extract was then partitioned with CH_2Cl_2 and water (1:1, v/v), and a CH_2Cl_2 extract (28.3 g) was obtained. The CH_2Cl_2-soluble part showed inhibitory activity against A549, MDA-MB-231, MCF7 and HepG2 cells ($IC_{50} < 20$μg/ml). Further fractionation of the CH_2Cl_2 extract was carried out by open liquid chromatography on silica gel (1000 ml; 0.063–0.200 mm) using gradients of CH_2Cl_2–MeOH, which yielded 18 fractions.

Fraction 6 (1.27 g) was fractionated on Sephadex LH-20 (diameter: 3 cm, length: 44 cm; $CHCl_3$–MeOH = 1:3), yielding six fractions. The fourth fraction (346 mg) was purified on a silica gel column (120 ml; 40–63 μm) eluted

with *n*-hexane–EtOAc (10:1, v/v) to obtain compound **16** (8.80 mg). Fraction 7 (3.90 g) was further fractionated into 13 fractions by silica gel cc (350 ml; 40–63 μm) using $CHCl_3$ as the eluent. The third fraction afforded compound **1** (761 mg).

The more polar fraction 8 (755 mg) was subjected to a silica gel cc (113 ml; 40–63 μm) using *n*-hexane–EtOAc (3:1, v/v) as eluant with an increasing ratio of EtOAc to obtain 11 fractions. Crystals precipitated from fraction 8-4 (15.9 mg), and addition of MeOH afforded compound **2** (3.40 mg). Subfraction 8-6 (253 mg) was divided into nine fractions on a silica gel column (108 ml; 40–63 μm) with $CHCl_3$ as the eluent. Subfraction 8-6-3 was purified on a preparative recycling HPLC system using a C_{30} column (250 × 21.2 mm) and H_2O–MeOH (20/80; flow rate: 3 ml/min) as the solvent system, which afforded compounds **3** (10.6 mg), **17** (12.7 mg) and **4** (25.2 mg). Subfraction 8-8 (116 mg) was subjected to silica gel cc (72 ml; 40–63 μm) eluting with *n*-hexane–$CHCl_3$ (1:5, v/v) and subsequently a Discovery column (250 × 10 mm) using H_2O–MeOH (20/80; flow rate: 2 ml/min) as the solvent system to give compound **5** (1.60 mg). Compound **6** (5.30 mg) was isolated from subfraction 8-10 (26.8 mg) on a Discovery column (250 × 10 mm) using H_2O–MeOH (25/75; flow rate: 2 ml/min) as the solvent system.

Fraction 10 (582 mg) was subjected to Sephadex LH-20 (diameter: 3 cm, length: 28 cm; $CHCl_3$–MeOH = 1:3) chromatography and then subfraction 10-3 (304 mg) was applied to a Sephadex LH-20 (diameter: 2.5 cm, length: 35 cm; *n*-hexane–EtOAc = 1:1) column. Subfraction 10-3-4 was purified with a Hypersil ODS column (250 × 21.2 mm) using H_2O–MeOH (40/60; flow rate: 3 ml/min) as the eluent. Compounds **7** (4.30 mg), **8** (4.20 mg), **9** (7.80 mg), **10** (4.40 mg), **11** (66.6 mg), and **15** (8.60 mg) were obtained.

Fraction 11 (457 mg) was purified further using Sephadex LH-20 (diameter: 3 cm, length: 41 cm; $CHCl_3$–MeOH = 1:3), subfraction 11-3 (197 mg) with Sephadex LH-20 (diameter: 2.5 cm, length: 30 cm; EtOAc–MeOH = 1:1), and subfraction 11-3-2 (150 mg) on a silica gel column (69 ml; 40–63 μm) using $CHCl_3$–MeOH (30:1, v/v) with increasing ratio of MeOH to obtain compound **12** (47.7 mg). Fraction 12 (146 mg) was subjected to Sephadex LH-20 (diameter: 2.5 cm, length: 32 cm; $CHCl_3$–MeOH = 1:3) cc, and subfraction 12-5 was treated with MeOH to afford compound **13** (2.1 mg). Fraction 13 (352 mg) was fractionated into six subfractions by Sephadex LH-20 (diameter: 3 cm, length: 44 cm; $CHCl_3$–MeOH = 1:1) chromatography. The fifth subfraction (67.1 mg) afforded compound **14** (37.6 mg) after silica gel cc (37 ml; 40–63 μm) using $CHCl_3$–MeOH (30:1, v/v).

3.4. Compound characterization

3.4.1. Gelomulide K (*1*)

Colorless needles (761 mg); m.p. 133–134 °C; $[\alpha]_D^{25}$ − 94.3 ($CHCl_3$; *c* 0.308); CD: $\Delta\varepsilon_{251.5}$ +5.44, $\Delta\varepsilon_{209.0}$ −12.97 (MeOH; *c* 0.1 mg/ml); UV λ_{max}^{MeOH} nm (log ε): 222 (4.11); IR (neat) ν_{max} 2949, 1759, 1720, 1452, 1376, 1240, 1026, 775 cm^{-1}; for ^1H and ^{13}C NMR (C_5D_5N) spectra, see Tables 1 and 2; HRESIMS *m/z* 395.1835 (calcd. for $C_{22}H_{28}O_5$ + Na, 395.1834).

3.4.2. Gelomulide L (*2*)

Colorless needles (3.40 mg); 230–231 °C (decom.; shrinked and turned into brown); $[\alpha]_D^{26}$ − 29.2 ($CHCl_3$; *c* 0.166); CD: $\Delta\varepsilon_{247.3}$ +3.69, $\Delta\varepsilon_{210.2}$ −8.67 (MeOH; *c* 0.1 mg/ml); UV λ_{max}^{MeOH} nm (log ε): 229 (3.74); IR (neat) ν_{max} 2916, 1775, 1730, 1454, 1373, 1238, 1027, 972, 760 cm^{-1}; for ^1H and ^{13}C NMR ($CDCl_3$) spectra, see Tables 1 and 2; HRESIMS *m/z* 453.1887 (calcd. for $C_{24}H_{30}O_7$ + Na, 453.1889).

3.4.3. Gelomulide M (*3*)

White amorphous (10.6 mg); m.p. 102–103 °C; $[\alpha]_D^{25}$ − 67.8 ($CHCl_3$; *c* 0.305); CD: $\Delta\varepsilon_{251.2}$ +4.18, $\Delta\varepsilon_{213.1}$ −10.52 (MeOH; *c* 0.1 mg/ml); UV λ_{max}^{MeOH} nm (log ε): 226 (3.80); IR (neat) ν_{max} 2962, 1759, 1738, 1454, 1372, 1239, 1030, 750 cm^{-1}; for ^1H and ^{13}C NMR (C_5D_5N) spectra, see Tables 1 and 2; HRESIMS *m/z* 453.1890 (calcd. for $C_{24}H_{30}O_7$ + Na, 453.1889).

3.4.4. Gelomulide N (*4*)

White amorphous (25.2 mg); m.p. 175–176 °C; $[\alpha]_D^{26}$ + 26.4 ($CHCl_3$; *c* 0.303); CD: $\Delta\varepsilon_{252.3}$ +6.41, $\Delta\varepsilon_{211.5}$ −14.92 (MeOH; *c* 0.1 mg/ml); UV λ_{max}^{MeOH} nm (log ε): 229 (3.89); IR (neat) ν_{max} 2955, 1759, 1737, 1448, 1374, 1246, 1020, 751 cm^{-1}; for ^1H and ^{13}C NMR (C_5D_5N) spectra, see Tables 1 and 2; HRESIMS *m/z* 455.2048 (calcd. for $C_{24}H_{32}O_7$ + Na, 455.2046).

3.4.5. Gelomulide O (*5*)

Colorless needles (1.60 mg); m.p. 221–222 °C; $[\alpha]_D^{27}$ − 7.9 ($CHCl_3$; *c* 0.138); CD: $\Delta\varepsilon_{252.5}$ +3.79, $\Delta\varepsilon_{209.1}$ −7.76 (MeOH; *c* 0.1 mg/ml); UV λ_{max}^{MeOH} nm (log ε): 221 (4.05); IR (neat) ν_{max} 2956, 1759, 1731, 1437, 1372, 1258, 1055, 1023, 755 cm^{-1}; for ^1H and ^{13}C NMR (C_5D_5N) spectra, see Tables 1 and 2; HRESIMS *m/z* 455.2047 (calcd. for $C_{24}H_{32}O_7$ + Na, 455.2046).

3.4.6. Gelomulide P (*6*)

White amorphous (5.30 mg); m.p. 232–233 °C; $[\alpha]_D^{24}$ + 11.2 ($CHCl_3$; *c* 0.427); CD: $\Delta\varepsilon_{251.2}$ +4.41, $\Delta\varepsilon_{212.9}$ −10.19 (MeOH; *c* 0.1 mg/ml); UV λ_{max}^{MeOH} nm (log ε): 220 (3.84); IR (neat) ν_{max} 3495, 2953, 1746, 1372, 1242, 1029, 750 cm^{-1}; for ^1H and ^{13}C NMR (C_5D_5N) spectra, see Tables 1 and 2; HRESIMS *m/z* 413.1942 (calcd. for $C_{22}H_{30}O_6$ + Na, 413.1940).

3.4.7. Gelomulide Q (*7*)

White amorphous (4.30 mg); m.p. 143–144 °C; $[\alpha]_D^{25}$ − 118.6 ($CHCl_3$; *c* 0.215); CD: $\Delta\varepsilon_{254.2}$ +1.54, $\Delta\varepsilon_{218.1}$ −11.58 (MeOH; *c* 0.1 mg/ml); UV λ_{max}^{MeOH} nm (log ε): 217 (4.12); IR (neat) ν_{max} 3470, 2960, 1734, 1371, 1240, 1022,

750 cm^{-1}; for ^1H and ^{13}C NMR ($CDCl_3$) spectra, see Tables 3 and 4; HRESIMS *m/z* 471.1995 (calcd. for $C_{24}H_{32}O_8 + Na$, 471.1994).

3.4.8. Gelomulide R (**8**)

White amorphous (4.20 mg); m.p. 153–154 °C; $[\alpha]_D^{24}$ −60.3 ($CHCl_3$; *c* 0.333); CD: $\Delta\varepsilon_{261.4}$ +1.53, $\Delta\varepsilon_{220.0}$ −12.10 (MeOH; *c* 0.1 mg/ml); UV λ_{max}^{MeOH} nm (log ε): 218 (3.98); IR (neat) ν_{max} 3446, 2927, 1734, 1733, 1373, 1250, 1022, 754 cm^{-1}; for ^1H and ^{13}C NMR (C_5D_5N) spectra, see Tables 3 and 4; HRESIMS *m/z* 473.2149 (calcd. for $C_{24}H_{34}O_8 + Na$, 473.2151).

3.4.9. Gelomulide S (**9**)

White amorphous (7.80 mg); m.p. 137–138 °C; $[\alpha]_D^{24}$ − 22.4 ($CHCl_3$; *c* 0.254); CD: $\Delta\varepsilon_{253.9}$ +1.28, $\Delta\varepsilon_{217.3}$ −11.07 (MeOH; *c* 0.1 mg/ml); UV λ_{max}^{MeOH} nm (log ε): 218 (4.03); IR (neat) ν_{max} 3442, 2968, 1734, 1375, 1248, 1028, 756 cm^{-1}; for ^1H and ^{13}C NMR (C_5D_5N) spectra, see Tables 3 and 4; HRESIMS *m/z* 473.2154 (calcd. for $C_{24}H_{34}O_8 + Na$, 473.2151).

3.4.10. Gelomulide T (**10**)

Colorless needles (4.40 mg); 238–239 °C (decom.; shrinked and turned into brown); $[\alpha]_D^{27}$ − 111.6 ($CHCl_3$; *c* 0.134); CD: $\Delta\varepsilon_{252.3}$ +1.16, $\Delta\varepsilon_{218.7}$ − 10.93 (MeOH; *c* 0.1 mg/ml); UV λ_{max}^{MeOH} nm (log ε): 217 (4.04); IR (neat) ν_{max} 3469, 3296, 2929, 1766, 1709, 1373, 1236, 1092, 1014, 960, 758 cm^{-1}; for ^1H and ^{13}C NMR (C_5D_5N) spectra, see Tables 3 and 4; HRESIMS *m/z* 471.1995 (calcd. for $C_{24}H_{32}O_8 + Na$, 471.1995).

3.4.11. Gelomulide U (**11**)

White amorphous (66.6 mg); m.p. 243–244 °C; $[\alpha]_D^{26}$ −218.5 ($CHCl_3$; *c* 0.314); CD: $\Delta\varepsilon_{251.5}$ +0.91, $\Delta\varepsilon_{220.0}$ −14.66 (MeOH; *c* 0.1 mg/ml); UV λ_{max}^{MeOH} nm (log ε): 220 (4.57); IR (neat) ν_{max} 3444, 2962, 1738, 1732, 1372, 1243, 1023, 975, 757 cm^{-1}; for ^1H and ^{13}C NMR (C_5D_5N) spectra, see Tables 3 and 4; HRESIMS *m/z* 413.1939 (calcd. for $C_{22}H_{30}O_6 + Na$, 413.1940).

3.4.12. Gelomulide V (**12**)

White amorphous (47.7 mg); m.p. 210–213 °C; $[\alpha]_D^{26}$ − 18.2 ($CHCl_3$; *c* 0.312); CD: $\Delta\varepsilon_{250.6}$ +1.59, $\Delta\varepsilon_{220.0}$ −13.37 (MeOH; *c* 0.1 mg/ml); UV λ_{max}^{MeOH} nm (log ε): 223 (3.82); IR (neat) ν_{max} 3289, 2923, 1720, 1718, 1275, 1032, 745 cm^{-1}; for ^1H and ^{13}C NMR (C_5D_5N) spectra, see Tables 3 and 4; HRESIMS *m/z* 429.1891 (calcd. for $C_{22}H_{30}O_7 + Na$, 429.1889).

3.4.13. Gelomulide W (**13**)

White amorphous (2.10 mg); m.p. 227–228 °C; $[\alpha]_D^{27}$ − 44.6 ($CHCl_3$; *c* 0.074); CD: $\Delta\varepsilon_{249.5}$ +1.39, $\Delta\varepsilon_{220.4}$ −7.05 (MeOH; *c* 0.1 mg/ml); UV λ_{max}^{MeOH} nm (log ε): 225 (4.01); IR (neat) ν_{max} 3326, 2921, 1738, 1713, 1666, 1074, 794 cm^{-1}; for ^1H and ^{13}C NMR (C_5D_5N) spectra, see Tables 3 and 4; HRESIMS *m/z* 385.1625 (calcd. for $C_{20}H_{26}O_6 + Na$, 358.1627).

3.4.14. Gelomulide X (**14**)

White amorphous (37.6 mg); m.p. 165–166 °C; $[\alpha]_D^{26}$ − 83.0 ($CHCl_3$; *c* 0.318); CD: $\Delta\varepsilon_{260.3}$ +1.21, $\Delta\varepsilon_{219.5}$ −11.06 (MeOH; *c* 0.1 mg/ml); UV λ_{max}^{MeOH} nm (log ε): 223 (3.81); IR (neat) ν_{max} 3406, 2922, 1737, 1012, 758 cm^{-1}; for ^1H and ^{13}C NMR (C_5D_5N) spectra, see Tables 3 and 4; HRESIMS *m/z* 371.1832 (calcd. for $C_{20}H_{28}O_5 + Na$, 371.1834).

3.4.15. Compound **15**

White amorphous (8.60 mg); 199–200 °C (decom.; shrinked and turned into brown); $[\alpha]_D^{26}$ − 27.8 ($CHCl_3$; *c* 0.289) [m.p. 212–216 °C; $[\alpha]_D^{28}$ + 133 ($CHCl_3$; *c* 0.003) (Choudhary et al., 2004)]; CD: $\Delta\varepsilon_{254.8}$ +1.16, $\Delta\varepsilon_{219.5}$ −10.36 (MeOH; *c* 0.1 mg/ml); UV λ_{max}^{MeOH} nm (log ε): 217 (3.92); IR (neat) ν_{max} 3475, 3376, 2924, 1748, 1731, 1684, 1369, 1260, 1092, 1021, 804 cm^{-1}; for ^1H and ^{13}C NMR (C_5D_5N) spectra, see Tables 3 and 4; HRESIMS *m/z* 427.1732 (calcd. for $C_{22}H_{28}O_7 + Na$, 427.1733).

3.4.16. Gelomulide A (**16**)

Colorless needles (8.80 mg); m.p. 221–222 °C; $[\alpha]_D^{26}$ + 46.6 ($CHCl_3$; *c* 0.262) [m.p. 239–248 °C; $[\alpha]_D^{28}$ + 105 ($CHCl_3$; *c* 0.003) (Choudhary et al., 2004)]; CD: $\Delta\varepsilon_{247.6}$ +4.85, $\Delta\varepsilon_{212.8}$ −10.61 (MeOH; *c* 0.1 mg/ml); UV λ_{max}^{MeOH} nm (log ε): 222 (4.07); IR (neat) ν_{max} 2949, 1759, 1720, 1452, 1375, 1248, 1178, 1095, 1024, 979, 765 cm^{-1}; for ^1H and ^{13}C NMR ($CDCl_3$) spectra, see Tables 1 and 2; HRESIMS *m/z* 375.2170 (calcd. for $C_{22}H_{30}O_5 + H$, 375.2171).

3.4.17. Gelomulide G (**17**)

White amorphous (12.7 mg); m.p. 100–101 °C; $[\alpha]_D^{25}$ + 42.7 ($CHCl_3$; *c* 0.304) [m.p. 207–211 °C; $[\alpha]_D^{28}$ + 96.6 ($CHCl_3$; *c* 0.003) (Choudhary et al., 2004)]; CD: $\Delta\varepsilon_{246.5}$ +5.31, $\Delta\varepsilon_{211.8}$ −10.32 (MeOH; *c* 0.1 mg/ml); UV λ_{max}^{MeOH} nm (log ε): 220 (4.15); IR (neat) ν_{max} 2947, 1759, 1731, 1444, 1373, 1243, 1030, 753 cm^{-1}; for ^1H and ^{13}C NMR (C_5D_5N) spectra, see Tables 1 and 2; HRESIMS *m/z* 455.2049 (calcd. for $C_{24}H_{32}O_7 + Na$, 455.2046).

3.4.18. X-ray diffraction analyses of compound **4**

Colorless crystals of **4** were obtained by recrystallization (100% MeOH). Crystallographic data for the structural analysis have been deposited with the Cambridge Crystallographic Data Centre (deposition number CCDC 615561). These data can be obtained free of charge via http://www.ccdc.cam.ac.uk/conts/retrieving.html (or from the CCDC, 12 Union Road, Cambridge CB2 1EZ, UK; fax: +44 1223 336 033; e-mail:deposit@ccdc.camac.uk).

3.5. (*R*)- and (*S*)-MTPA derivatives of **12** and **14**

Preparation of the (*R*)-MTPA ester derivative of **12** was carried out by a convenient Mosher ester procedure

(Ohtani et al., 1991). Compound **12** (4.13 mg, 0.01 mmol) was transferred into a clean NMR tube, dried completely under vacuum, and maintained under N_2 gas. C_5D_5N (0.5 mL) and (*S*)-(+)-α-methoxy-α-(trifluoromethyl)-phenyl-acetyl chloride (5.14 mg, 0.02 mmol) were added immediately into the NMR tube, and the NMR tube was shaken carefully to mix the sample and MTPA chloride. The mixture was reacted for 24 h at room temperature, and then the NMR spectra were recorded. The (*R*)-MTPA ester of **14** and (*S*)-MTPA esters of **12** and **14** were prepared similarly.

*3.5.1. (S)-MTPA ester of **12***

^{1}H NMR (C_5D_5N, 400 MHz) δ 5.53 (H-1, *d*), 6.12 (H-2, *dd*), 5.79 (H-3, *d*), 2.38 (H-5, *dd*), 2.11 (H-6β, *ddd*), 5.72 (H-7, *t*), 2.7 (H-9, *d*), 2.01 (H-11β, *ddd*), 5.64 (H-12, *ddd*), 5.11 (H-14, *s*), 1.77 (Me-17, *s*), 0.90 (Me-18, *s*), 1.01 (Me-19, *s*), 1.55 (Me-20, *s*), 1.95 (OCO*Me*, *s*).

*3.5.2. (R)-MTPA ester of **12***

^{1}H NMR (C_5D_5N, 400 MHz) δ 5.49 (H-1, *d*), 6.17 (H-2, *dd*), 5.73 (H-3, *d*), 2.30 (H-5, *dd*), 2.07 (H-6β, *ddd*), 5.76 (H-7, *t*), 3.0 (H-9, *d*), 2.17 (H-11β, *ddd*), 5.69 (H-12, *ddd*), 5.15 (H-14, *s*), 1.79 (Me-17, *s*), 0.85 (Me-18, *s*), 0.87 (Me-19, *s*), 1.57 (Me-20, *s*), 1.92 (OCO*Me*, *s*).

*3.5.3. (S)-MTPA ester of **14***

^{1}H NMR (C_5D_5N, 400 MHz) δ 5.54 (H-1, *d*), 6.12 (H-2, *dd*), 5.79 (H-3, *d*), 1.91 (H-5, *dd*), 1.70 (H-6α, *m*), 2.36 (H-6β, *dddd*), 1.98 (H-7α, *ddd*), 2.59 (H-7, *ddd*), 2.65 (H-9, *d*), 2.65 (H-11α, *dd*), 2.08 (H-11β, *ddd*), 5.63 (H-12, *ddd*), 5.07 (H-14, *s*), 1.83 (Me-17, *s*), 0.93 (Me-18, *s*), 1.05 (Me-19, *s*), 1.56 (Me-20, *s*).

*3.5.4. (R)-MTPA ester of **14***

^{1}H NMR (C_5D_5N, 400 MHz) δ 5.50 (H-1, *d*), 6.13 (H-2, *dd*), 5.70 (H-3, *d*), 1.79 (H-5, *dd*), 1.64 (H-6α, *m*), 2.34 (H-6β, *dddd*), 1.97 (H-7α, *ddd*), 2.65 (H-7, *ddd*), 2.73 (H-9, *d*), 2.77 (H-11α, *dd*), 2.23 (H-11β, *ddd*), 5.65 (H-12, *ddd*), 5.11 (H-14, *s*), 1.88 (Me-17, *s*), 0.86 (Me-18, *s*), 0.98 (Me-19, *s*), 1.56 (Me-20, *s*).

3.6. Cytotoxicity assay

Fractions and isolates were tested against lung (A549), breast (MEA-MB-231 and MCF7), and liver (HepG2) cancer cell lines using established colorimetric MTT assay protocols (Mosmann, 1983). Doxorubicin was used as a positive control. Freshly trypsinized cell suspensions were seeded in 96-well microtiter plates at densities of 5000–10,000 cells per well with tested compounds added from DMSO stock solution. After 3 days in culture, attached cells were incubated with MTT (0.5 mg/mL, 2 h) and subsequently solubilized in DMSO. The absorbance was measured at 550 nm using a microplate reader. The IC_{50} is the concentration of agent that reduced cell growth by 50% under the experimental conditions.

Acknowledgements

We gratefully acknowledge the financial support for this project from the National Science Council and National Science Technology Program/Biotechnology and Pharmaceuticals, and National Sun Yat-Sen University-Kaohsiung Medical University Joint Research Center, Taiwan. Thanks are also due to partial support from NIH Grant CA17625 awarded to K.H.L.

Appendix A. Supplementary data

Supplementary data associated with this article can be found, in the online version, at doi:10.1016/j.phytochem.2007.07.005.

References

Beecham, A.F., 1972. The CD of αβ-unsaturated lactones. Tetrahedron 28, 5543–5554.

Chakravarty, A.K., Pal, B.C., Guittet, E., Ahond, A., 1991. Structure of a new diterpene lactone from *Gelonium multiflorum* by 2D NMR. Indian J. Chem. Sect. B 30, 3–6.

Chen, L.A., Hsia, H.M., Kuo, N.F., Wang, C.W., Wang, S.M., Hsieh, K.C., 1993. Flora of Taiwan 3, 474.

Choudhary, M.I., Gondal, H.Y., Abbaskhan, A., Jahan, I.A., Parvez, M., Nahar, N., Atta-ur-Rahman, 2004. Revisiting diterpene lactones of *Suregada multiflora*. Tetrahedron 60, 7933–7941.

Das, B., Chakravarty, A.K., 1993. Three flavone glycosides from *Gelonium multiflorum*. Phytochemistry 33, 493–496.

Das, B., Chakravarty, A.K., Masuda, K., Suzuki, H., Ageta, H., 1994. A diterpenoid from roots of *Gelonium multiflorum*. Phytochemistry 37, 1363–1366.

Devon, T.K., Scott, A.I., 1972. Terpenes. Handbook of Naturally Occurring Compounds vol. II, 185–279.

Jahan, I.A., Nahar, N., Mosihuzzaman, M., Shaheen, F., Parween, Z., Atta-ur-Rahman, Choudhary, M.I., 2002. Novel diterpene lactones from *Suregada multiflora*. J. Nat. Prod. 65, 932–934.

Jahan, I.A., Nahar, N., Mosihuzzaman, M., Shaheen, F., Atta-ur-Rahman, Choudhary, M.I., 2004. Six new diterpenoids from *Suregada multiflora*. J. Nat. Prod. 67, 1789–1795.

Mosmann, T., 1983. Rapid colorimetric assay for cellular growth and survival: application to proliferation and cytotoxicity assays. J. Immunol. Methods 65, 55–63.

Nakanishi, K., Goto, T., Itô, S., Natori, S., Nozoe, S., 1974. Nat. Products Chem. 1, 185–312.

Ohtani, I., Kusumi, T., Kashman, Y., Kakisawa, H., 1991. High-field FT NMR application of Mosher's method. The absolute configurations of marine terpenoids. J. Am. Chem. Soc. 113, 4092–4096.

Parveen, N., Khan, N.U., 1987. Luteolin 7,4′-dimethyl ether 3′-glucoside from *Gelonium multiflorum*. Phytochemistry 26, 2130–2131.

Row, L.R., Rao, C.S., 1969. Crystalline constituents of Euphobiaceae: Part X—The triterpenes of *Gelonium multiflorum* bark. Indian J. Chem. 7, 207–209.

Sengupta, P., Khastgir, H.N., 1963. Terpenoids and related compounds—III: Bauerenol and multiflorenol from *Gelonium multiflorum* A. Juss. The structure of multiflorenol. Tetrahedron 19, 123–132.

Talapatra, S.K., Das, G., Talapatra, B., 1989. Stereostructures and molecular conformations of six diterpene lactones from *Gelonium multiflorum*. Phytochemistry 28, 1181–1185, and 3581–3582.

Talapatra, B., Das, G., Das, A.K., Biswas, K., Talapatra, S.K., 1998. Stereostructures and conformations of four diterpene lactones from *Gelonium multiflorum*. Phytochemistry 49, 1353–1360.